Inert Shell Effect on the Quantum Yield of Neodymium-Doped Near-Infrared Nanoparticles: The Necessary Shield in an Aqueous Dispersion

Artiom Skripka[¶], Antonio Benayas[#], Carlos D. S. Brites[#], Inocencio R. Martín[§†], Luís D. Carlos[#], and Fiorenzo Vetrone[¶]**

[¶]Centre Énergie, Matériaux et Télécommunications, Institut National de la Recherche Scientifique, Université du Québec, 1650 Boul. Lionel-Boulet, Varennes, QC, J3X 1S2, Canada

[#]Phantom-g, CICECO-Aveiro Institute of Materials, Department of Physics, University of Aveiro, Campus de Santiago, 3810-193 Aveiro, Portugal

[§]Departamento de Física, Universidad de La Laguna, Apdo. 456. E-38200 San Cristóbal de La Laguna, Santa Cruz de Tenerife, Spain

[†]Instituto Universitario de Materiales y Nanotecnología (IMN), Universidad de La Laguna, Apdo. 456, E-38200 San Cristóbal de La Laguna, Santa Cruz de Tenerife, Spain

***Corresponding authors:** lcarlos@ua.pt and vetrone@emt.inrs.ca

Table of Contents

Materials and Methods

Materials

Gd_2O_3 (REacton, 99.99+%), Nd_2O_3 (REacton, 99.99+%), trifluoroacetic acid (99%), 1-octadecene (ODE, 90%), oleic acid (OA, 90%) and sodium trifluoroacetate (98%) were purchased from Alfa Aesar (USA). All chemicals were used without further purification.

Precursor preparation

Lanthanide (Ln) trifluoroacetate precursors (2.5 mmol) for the synthesis of $NaGdF_4$:Nd^{3+} core LnNPs of different Nd^{3+} doping (0, 5, 12.5 and 25 mol%) were prepared by mixing stoichiometric quantities of Gd_2O_3 and Nd_2O_3 (total amount of oxides corresponding to 1.25 mmol) in each case with 5 mL trifluoroacetic acid and 5 mL of water in 50 mL three-neck round bottom flasks. The mixtures were refluxed under vigorous stirring at 80 ºC until the solutions became clear, at which point the temperature was decreased to 60 ºC for residual trifluoroacetic acid and water to evaporate. Gadolinium trifluoroacetate precursors for subsequent $NaGdF_4$ shelling were prepared in analogous fashion out of Gd_2O_3.

LnNP synthesis

LnNPs were prepared via thermal decomposition method, using the hot-injection approach.[1]

Core synthesis: An initial mixture of 12.5 mL each of OA and ODE, was prepared in a 100 mL three-neck round bottom flask (Solution A). Solution A was degassed under vacuum at 110 ºC for 15 min, after which it was back-filled with Ar and the temperature was raised to 315 ºC. Meanwhile, 2.5 mmol of sodium trifluoroacetate was added to the dried core precursors together with 7.5 mL each of OA and ODE (Solution B). Solution B was then degassed under vacuum at 125 ºC for 30 min. Once Solution A reached stable temperature, Solution B was injected into Solution A using a pump-syringe system (Harvard Apparatus Pump 11 Elite). For 0, 5, 12.5 and 25 mol% Nd^{3+}-doped core LnNPs, the injection rate was 1.40, 1.45, 1.50 and 1.50 mL/min, respectively. After 1 h of vigorous stirring at 315 ºC, the mixture was cooled down to room temperature. The synthesized core-only LnNPs were stored in Falcon centrifuge tubes (50 mL) for the subsequent shelling step.

Core shelling: Core/shell LnNPs were prepared by epitaxial growth of the shell on the preformed cores via the hot-injection approach. Approximately 0.3 mmol of core LnNPs were mixed in 100 mL three-neck round bottom flask together with equal parts of OA and ODE up to a total volume of 25 mL (Solution A). Separately, Solution B was prepared by mixing 1.25 mmol of sodium trifluoroacetate precursors together with 1.25 mmol of gadolinium trifluoroacetate and 7.5 mL each of OA and ODE. Both solutions were degassed under vacuum and magnetic stirring at 110 ºC for 30 min. After degassing, Solution A was back-filled with Ar and the temperature was raised to 310 ºC. Solution B was then injected into the reaction vessel containing Solution A

using the pump-syringe system at a 0.5 mL/min injection rate. After 1 h of reaction, the mixture was cooled to RT under Ar and magnetic stirring. Prior to washing steps, aliquots of the obtained core/shell LnNPs were sampled under electron transmission microscopy (TEM) for size.

Due to evaporation of impurities in the starting materials (such as OA and ODE) and reaction byproducts, as well as minor losses accrued from the intermediate steps of liquid handling, some errors would be introduced in the determination of exact core amounts that were subjected to shelling, which lead to lower than expected shell thickness for 0, 12.5 and 25 mol% Nd^{3+}-doped LnNPs. Hence, these LnNPs underwent secondary shelling step in an analogous way as described above, starting with ~0.15 mmol of initially formed core/shell LnNPs and introducing additional 0.65 mmol of sodium and gadolinium trifliuoroacetate precursors to obtain all LnNPs of similar size and shell thickness.

Final core-only and core/shell LnNPs were precipitated with ethanol and washed three times with hexane/ethanol (1/4 v/v in each case), followed by centrifugation (5400 RCF). Finally, all LnNPs were re-dispersed in hexane for further characterization and surface treatment.

Transfer to water via ligand removal

Ligand-free LnNPs were prepared via previously reported ligand removal procedure.[2] 50 mg of oleate-capped LnNPs dispersed in 25 mL of hexane were mixed together with 25 mL of distilled water of (pH ~3-4) and left under vigorous stirring for 3 h. The two phase (aqueous/organic) mixture was poured into the separatory funnel, and the aqueous phase containing the LnNPs was isolated. The LnNPs were then precipitated with acetone (1/3 v/v) via centrifugation at 7500 RPM for 30 min. The obtained pellet was re-dispersed in 25 mL of distilled water (pH ~3-4) and left under stirring for additional 2 h. LnNPs were then precipitated with acetone (1/3 v/v) via centrifugation at 7500 RPM for 30 min, and washed twice with a mixture of water/acetone (1/3 v/v). The ligand-free LnNPs were then re-dispersed in distilled water at an approximate 15 mg/mL concentration.

Structural characterization

The crystallinity and phase of the core-only and core/shell LnNPs were determined via X-ray powder diffraction (XRD) analysis with a Bruker D8 Advance Diffractometer using CuKα radiation. The morphology and size distribution of the core-only and core/shell LnNPs were investigated with a Philips Tecnai 12 transmission electron microscope (TEM). The particle size was determined from TEM images using ImageJ image analysis software with set size of at least 200 individual particles per sample. Ln^{3+} molar doping concentration was determined via inductively coupled plasma - optical emission spectroscopy (ICP-OES) with an Agilent Technologies 5100 ICP-OES spectrometer.

Optical characterization

Photoluminescence spectra and absolute photoluminescence quantum yield (PLQY) of all LnNPs were measured with a quantum yield measurement system Quantaurus-QY (C13534, Hamamatsu), equipped with a 150 W Xenon lamp coupled to a monochromator for wavelength discrimination, an integrating sphere as sample chamber and two multi-channel analyzers for signal detection in the visible and in the NIR spectral ranges. An 804 nm external laser diode (FC-808 5W, CNI Lasers) was used as the excitation source. The laser power is adjusted between 0.25-1.33 W (corresponding to 102-532 W/cm^2, considering the illumination area in the sample holder, 0.0025 cm^2, measured by the manufacturer) by controlling the laser diode current. All measurements were performed in quartz cuvettes of 1 cm optical path, filled with 2 mL of LnNPs at 15 mg/mL concentration. As a reference sample, the empty cuvette, the cuvette filled with hexane or water, and the cuvette containing undoped $NaGdF_4$ LnNPs dispersed in hexane or water were used. PLQY was calculated by the quotient between the emitted and absorbed photons by the sample. The equipment's software computes the PLQY using the user-defined wavelength integration ranges for excitation and emission. Three measurements were performed for each sample at each power density value and the mean value is reported. Final reported PLQY values are a mean of up to 33 individual measurements, considering 11 different excitation power densities studied, and three repetitions per each power density. According to the manufacturer, each measurement presents a relative systemic error of 10 %.

The photoluminescence decay curves were measured by exciting the colloidal dispersions of LnNPs with a 10 ns pulsed optical parametric oscillator (OPO) laser (EKSPLA/NT342/3/UVE) at 575 or 800 nm. Generated photoluminescence was focused on the entrance slit of a monochromator (Triax 180; grating - 600 lines/mm and 1 μm blaze) coupled to a NIR extended photomultiplier tube (Hamamatsu R406), and the electronic signal was registered with a digital oscilloscope (Lecroy WS424). Average decay time values were obtained from integrated area under the decay profiles:

$$\tau = \int_{t_0}^{\infty} \frac{I(t)dt}{I(0)}$$

XRD Patterns of $NaGdF_4$:Nd^{3+}/$NaGdF_4$ LnNPs

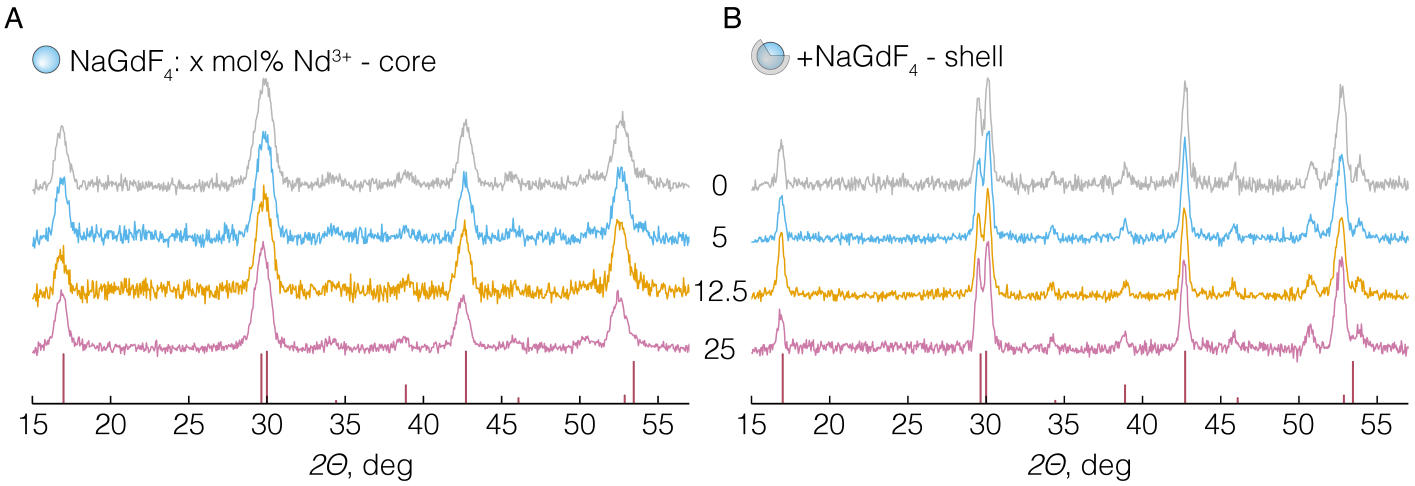

Figure S1. XRD patterns of core-only (A) and core/shell (B) $NaGdF_4$: x mol% Nd^{3+}/$NaGdF_4$ LnNPs (x = 0, 5, 12.5 and 25). Diffraction peaks of pure hexagonal $NaGdF_4$ are shown in red (PDF# 01-080-8787).

Summary of Structural and Morphological Properties of $NaGdF_4$:Nd^{3+}/$NaGdF_4$ LnNPs

Table S1. Overview of the structural and morphological characteristics of $NaGdF_4$:Nd^{3+}/$NaGdF_4$ LnNPs: nominal and actual doping in mol% (measured via ICP-OES with maximum relative error of 15%), core and core/shell size of LnNPs, and respective estimate of shell thickness. Although ICP-OES measurements detected trace amount of Nd^{3+} in undoped $NaGdF_4$ LnNPs, these LnNPs showed no photoluminescence (see Figure S3) and could be reliably used as the blank reference.

Ln^{3+} doping (nominal), mol%	Ln^{3+} doping (actual), mol%	core size, nm	core/shell size, nm	shell thickness, nm
$NaGdF_4$:Nd^{3+}/$NaGdF_4$				
0.0	**0.4**	**11.0 ± 0.7**	**26.9 ± 1.0**	**7.95 ± 1.22**
5.0	**5.1**	**12.4 ± 0.5**	**25.3 ± 0.7**	**6.45 ± 0.51**
12.5	**12.9**	**11.8 ± 0.8**	**26.2 ± 0.8**	**7.20 ± 0.84**
25.0	**25.6**	**11.1 ± 1.0**	**25.9 ± 1.0**	**7.40 ± 1.41**

Photoluminescence Decay of $NaGdF_4:Nd^{3+}/NaGdF_4$ LnNPs

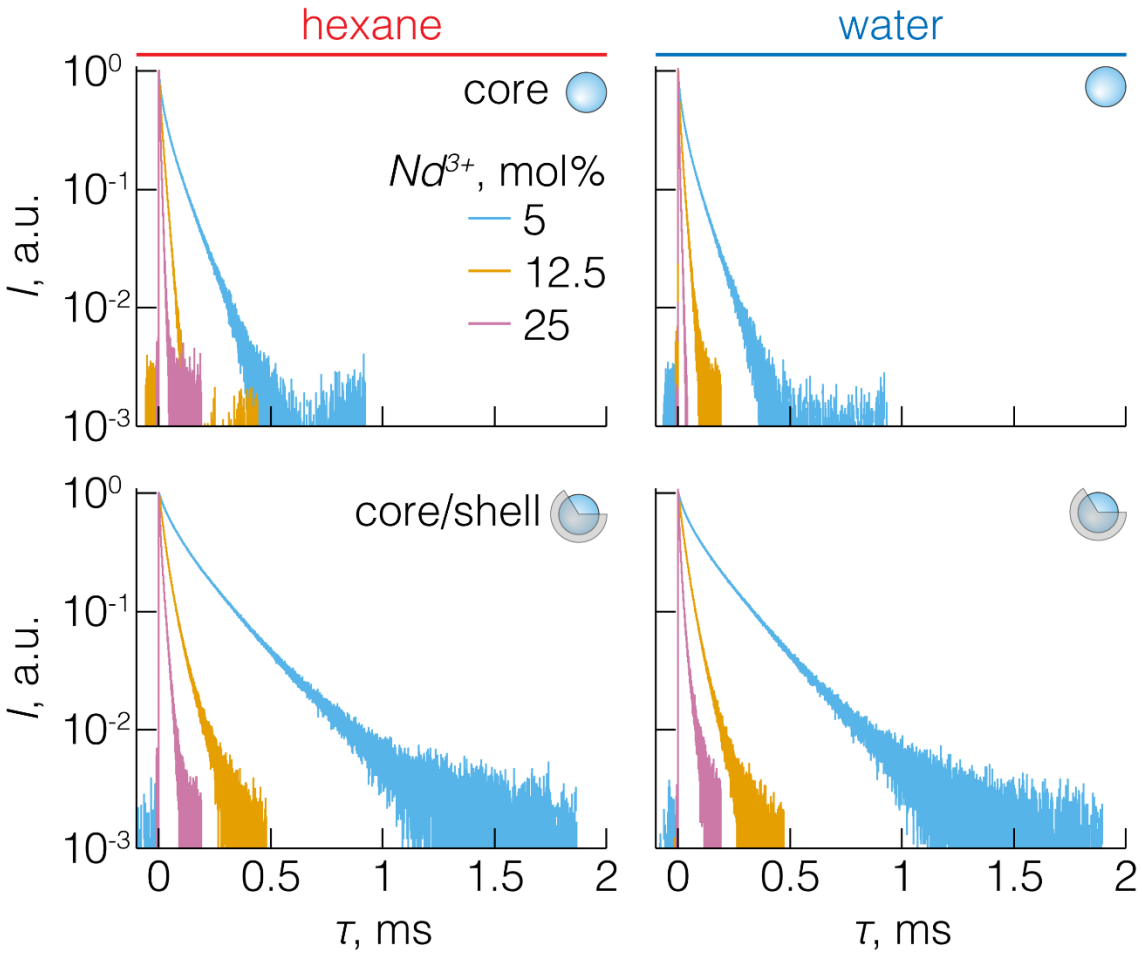

Figure S2. Normalized photoluminescence decay profiles of core-only (top) and core/shell (bottom) $NaGdF_4$: x mol% $Nd^{3+}/NaGdF_4$ LnNPs (x = 5, 12.5 and 25) dispersed in hexane (left) or water (right) under 800 nm laser excitation. Photoluminescence decay was measured from emission band around 885 nm ($^4F_{3/2} \rightarrow {}^4I_{9/2}$).

TEM Images of $NaGdF_4$/$NaGdF_4$ LnNPs

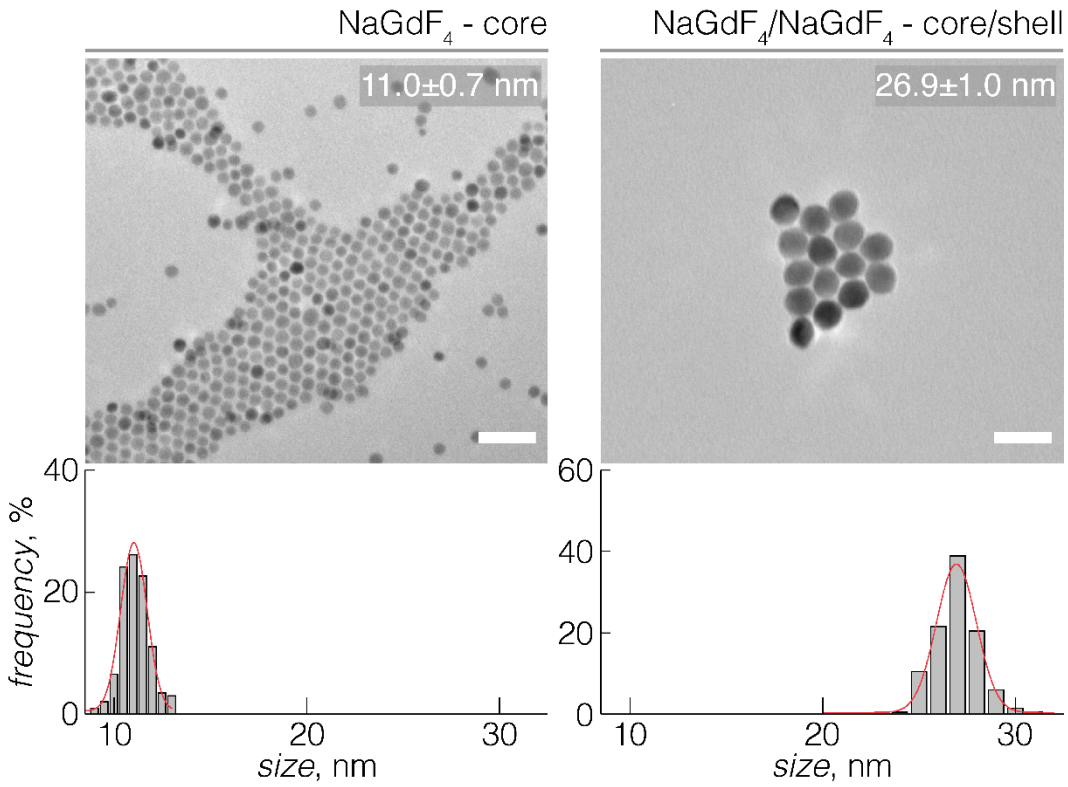

Figure S3. TEM images and size distributions of core-only and core/shell undoped $NaGdF_4$/$NaGdF_4$ LnNPs, used as blank reference in PLQY measurements.

Reference Spectrum of Blank LnNPs

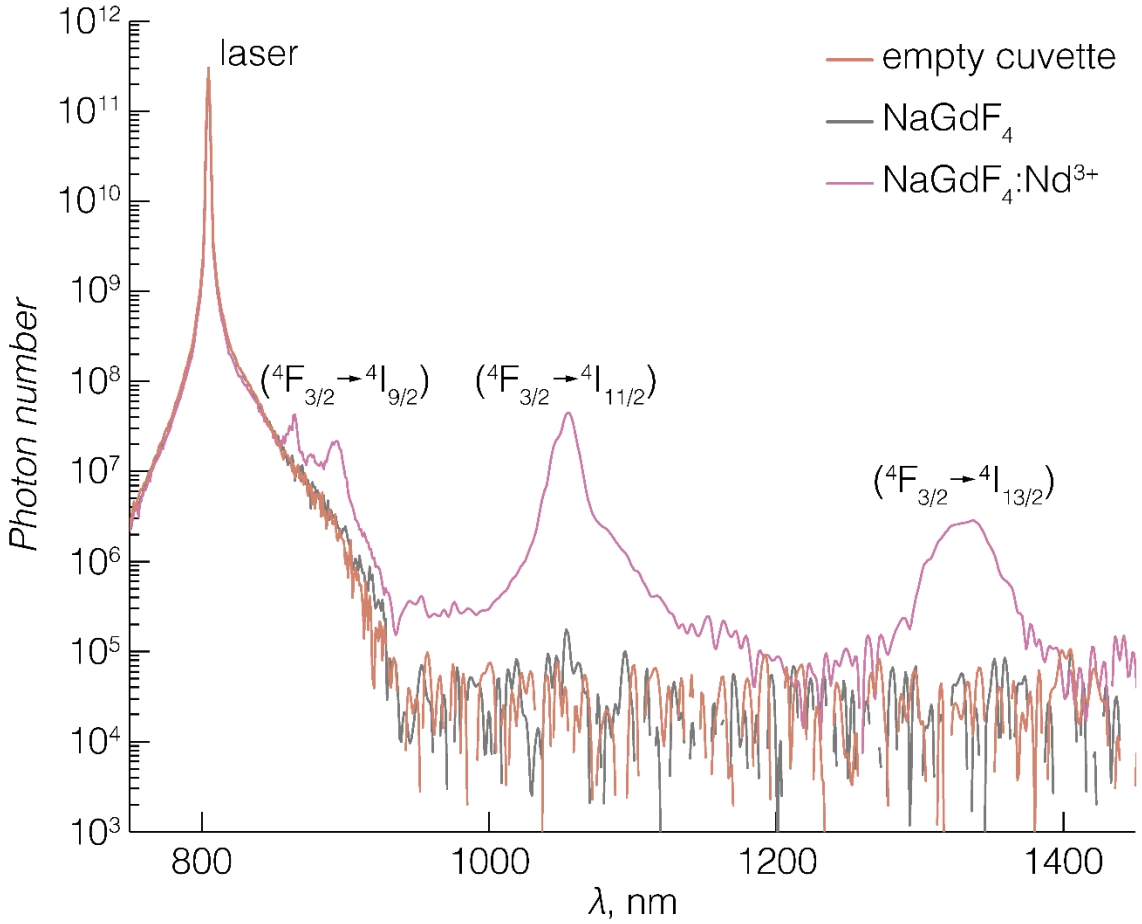

Figure S4. Reference spectra of empty cuvette and cuvette with undoped $NaGdF_4$ LnNPs dispersed in hexane, against photoluminescence spectra of $NaGdF_4$: 25 mol% Nd^{3+} LnNPs. Spectra measured at maximum excitation power density of 532 W/cm^2.

PLQY of $NaGdF_4$:Nd^{3+}/$NaGdF_4$ LnNPs

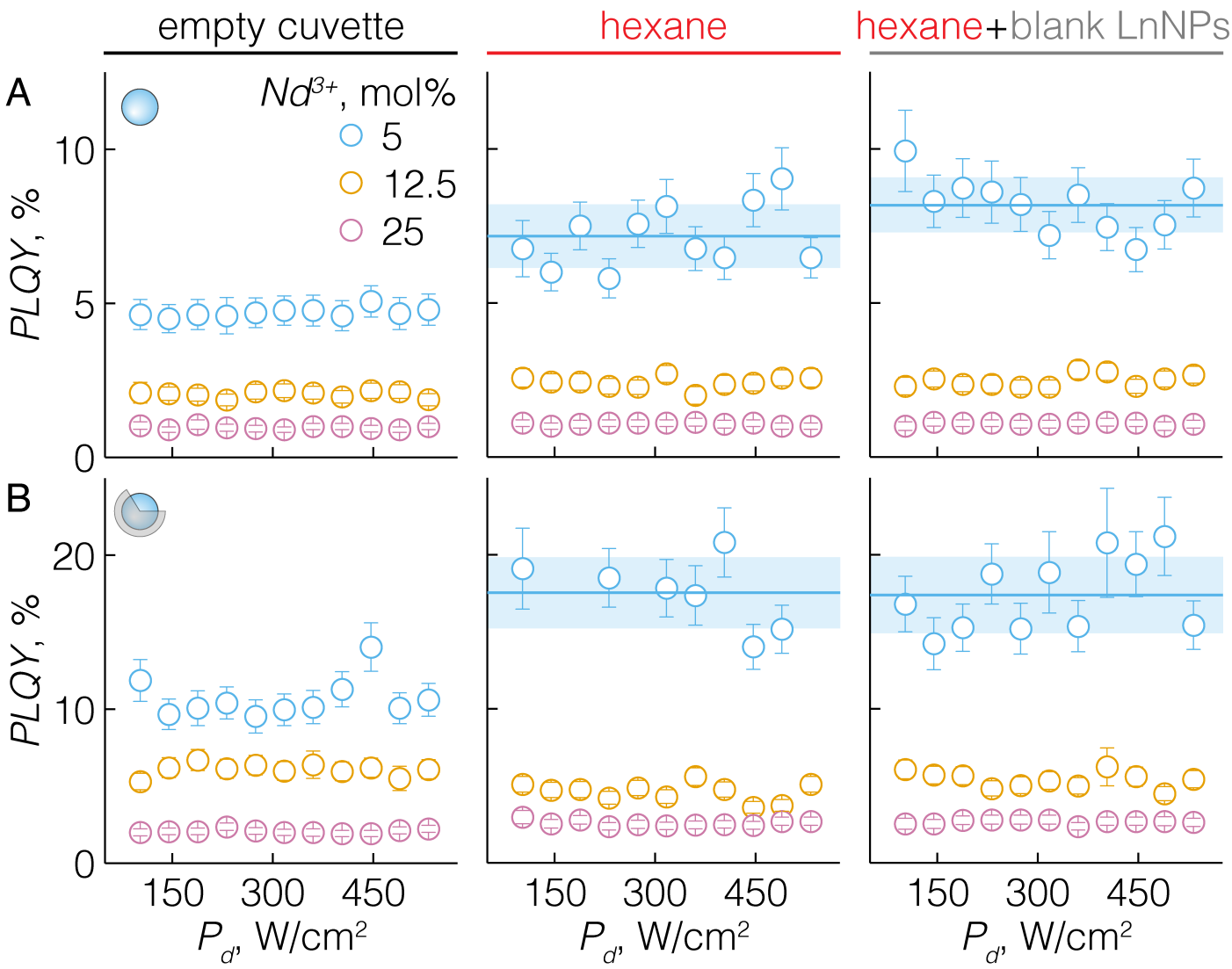

Figure S5. PLQY of core-only (A) and core/shell (B) $NaGdF_4$: x mol% Nd^{3+}/$NaGdF_4$ LnNPs (x = 5, 12.5 and 25) dispersed in hexane under 804 nm laser excitation of varying power density (P_d). PLQY was measured using an empty cuvette, cuvette filled with hexane, or cuvette filled with undoped (blank) LnNPs dispersed in hexane as references. Solid lines and shaded areas for certain 5 mol% Nd^{3+}-doped LnNPs represent average PLQY and standard deviation, respectively.

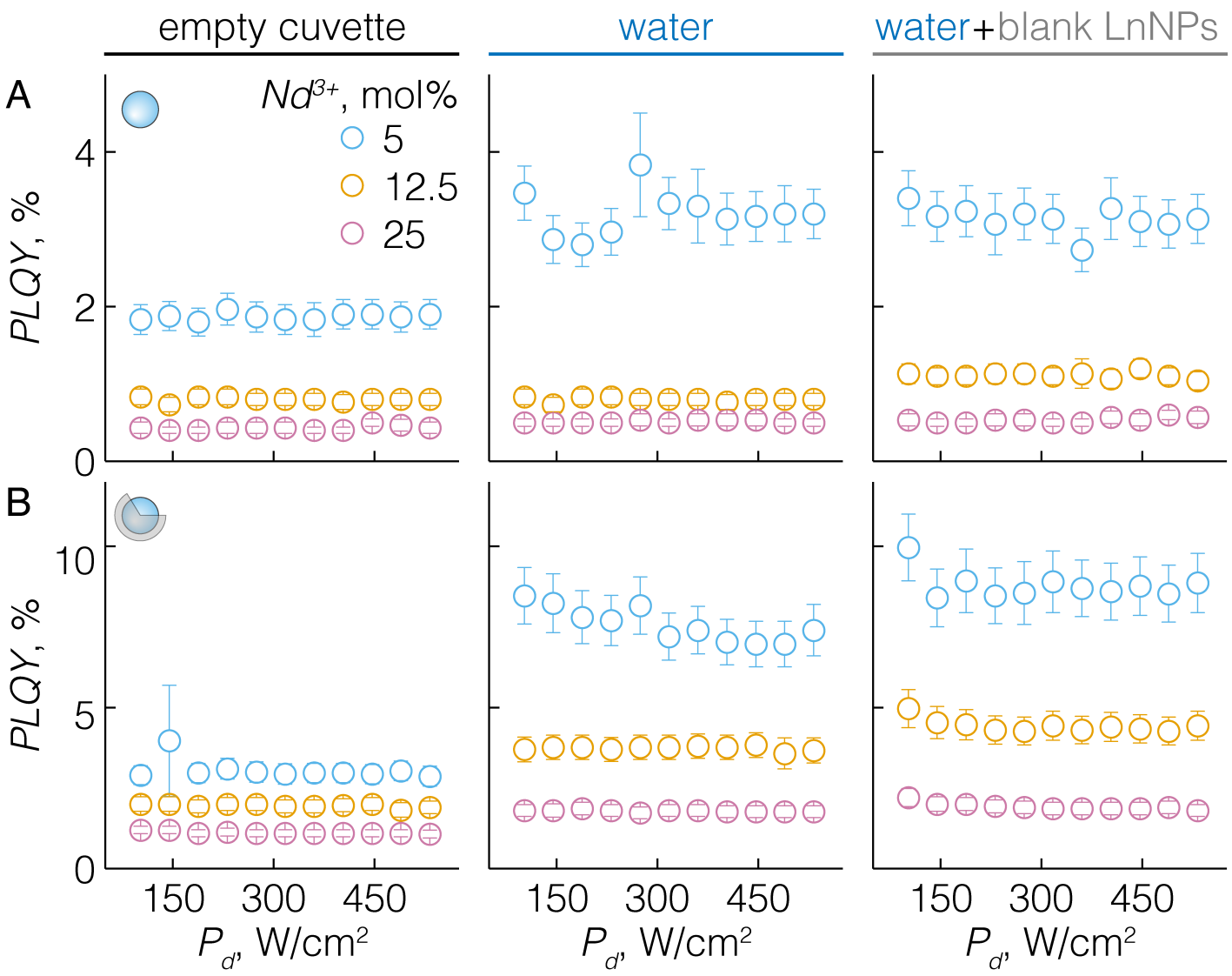

Figure S6. PLQY of core-only (A) and core/shell (B) $NaGdF_4$: x mol% Nd^{3+}/$NaGdF_4$ LnNPs (x = 5, 12.5 and 25) dispersed in water under 804 nm laser excitation of varying power density (P_d). PLQY was measured using an empty cuvette, cuvette filled with water, or cuvette filled with undoped (blank) LnNPs dispersed in water as references.

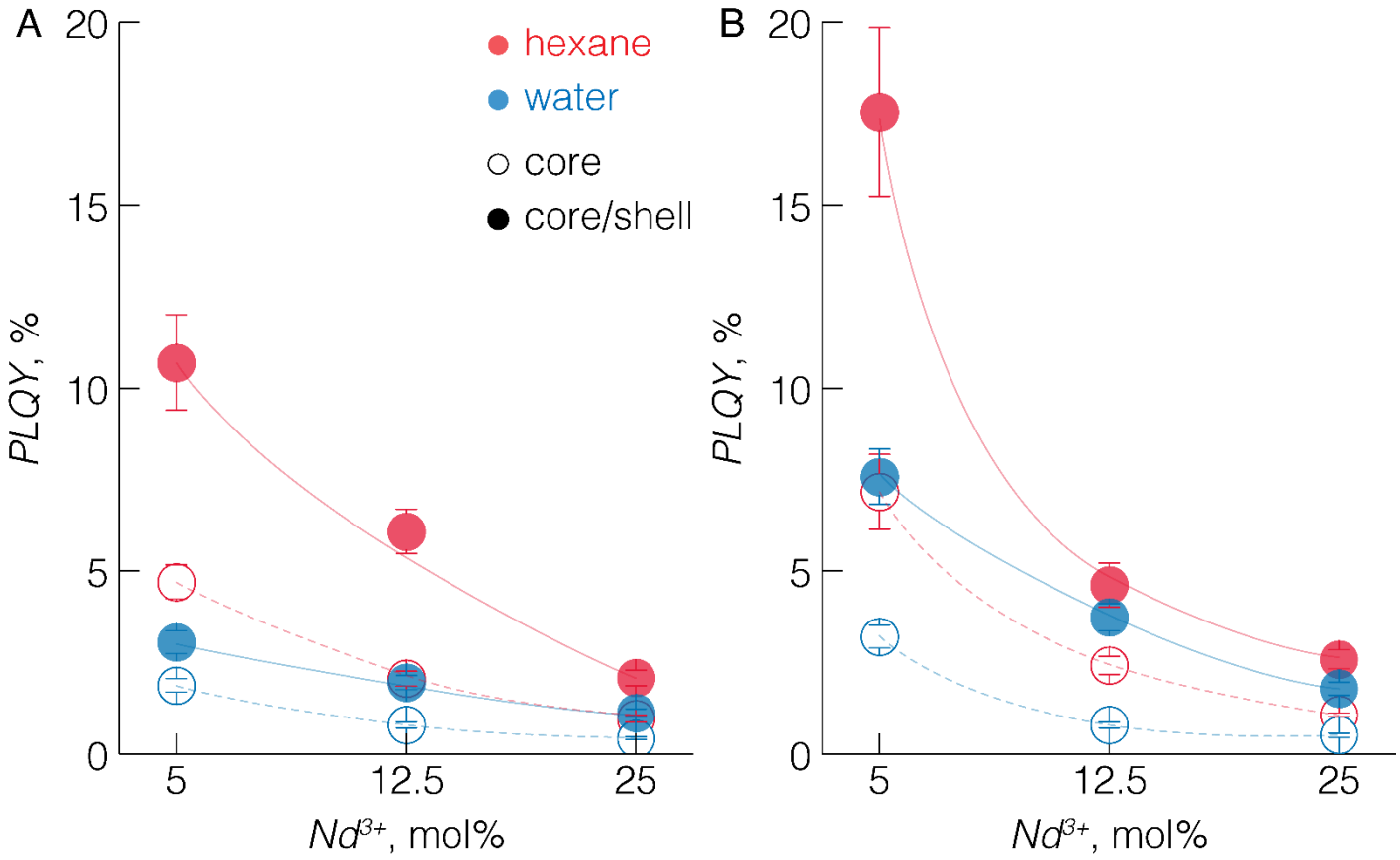

Figure S7. Average PLQY values of $NaGdF_4$: x mol% Nd^{3+}/$NaGdF_4$ LnNPs (x = 5, 12.5 and 25) under 804 nm excitation when dispersed in hexane (red data points) or water (blue) in their core-only or core/shell formulations. PLQY was measured using empty cuvette (A) or cuvette filled with respective media, hexane or water (B).

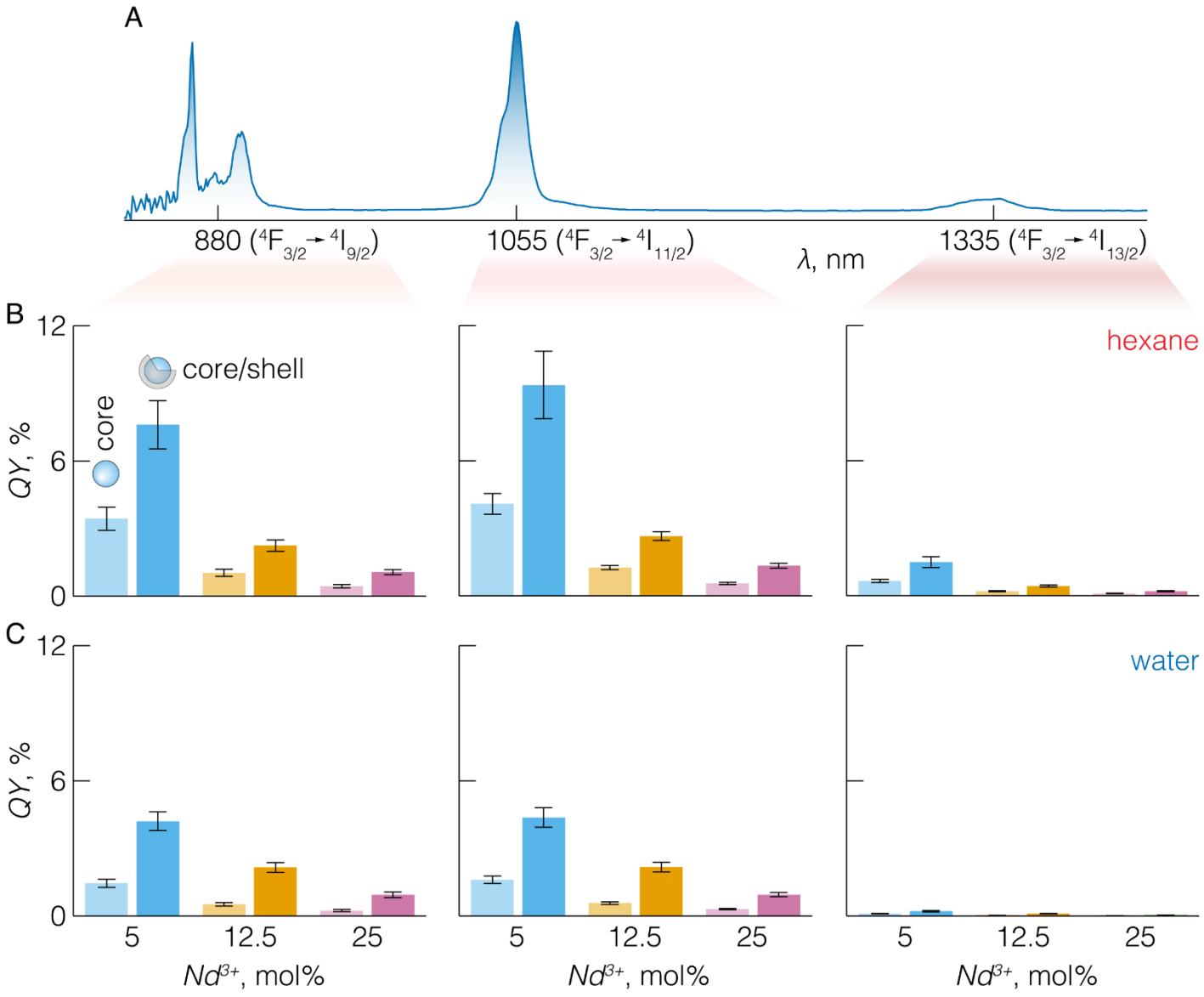

Figure S8. A – photoluminescence spectra of Nd^{3+}-doped LnNPs, and B, C – average PLQY values for each photoluminescence band of $NaGdF_4$: x mol% $Nd^{3+}/NaGdF_4$ LnNPs (x = 5, 12.5 and 25) under 804 nm excitation when dispersed in hexane (B) or water (C) in their core-only or core/shell formulations. PLQY was measured using and undoped (blank) LnNPs dispersed in respective media as a reference.

$^4F_{5/2}$ Excited State Quenching?

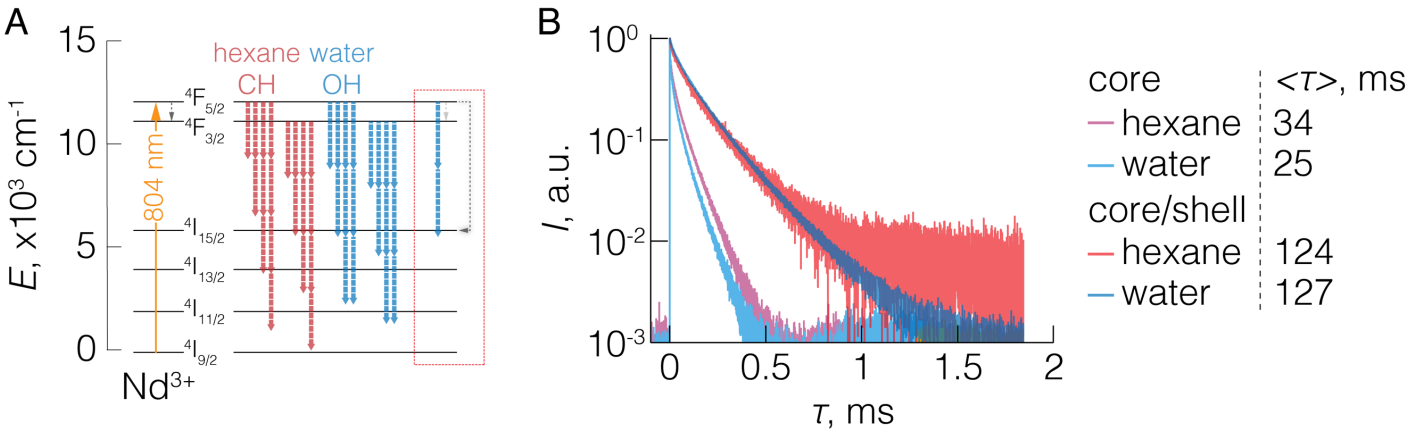

Figure S9. A – simplified energy level scheme of Nd^{3+} showing $^4I_{9/2} \rightarrow {}^4F_{5/2}$ excitation with 804 nm light, followed by population of the emissive $^4F_{3/2}$ excited state via non-radiative $^4F_{5/2} \rightarrow {}^4F_{3/2}$ decay. In the extended view media vibrations (CH ~ 2900 cm^{-1} for hexane and OH ~ 3400 cm^{-1} for water) are represented as multiphonon quenching modes for $^4F_{3/2}$ and $^4F_{5/2}$ excited states. Notably, near-resonant bridging of the $^4F_{5/2}$-$^4I_{15/2}$ energy gap is possible via multimodal vibrational quenching, but would require additional lattice phonon assistance to quench $^4F_{3/2}$ excited state directly. B - Normalized photoluminescence decay profiles of core-only and core/shell $NaGdF_4$: 5 mol% Nd^{3+}/$NaGdF_4$ LnNPs dispersed in hexane or water under 575 nm laser excitation. Photoluminescence decay was measured from emission band around 800 nm ($^4F_{5/2} \rightarrow {}^4I_{9/2}$). Average decay time values of each trace are indicated next to the legend.

Estimation of Nd^{3+} Number per LnNP

Hexagonal $NaGdF_4$ unit cell contains Z = 1.5 number of Ln^{3+} per cell, and its parameters are a = 6.02 Å and c = 3.60 Å. The unit cell volume V_{cell} is ~ 0.113 nm^3. Due to the estimation of only the diameter (d) of LnNPs from TEM images, LnNPs were considered as spheres for illustrative purposes of relative brightness change with doping amount. Given the volume (V_{LnNPs}) of LnNPs' core as:

$$V_{RENPs} = \frac{4}{3}\pi r^3$$

The number of Ln^{3+} dopants (#) per LnNPs' core is:

$$\# = \frac{V_{RENPs}}{V_{cell}} \times Z \times c(Ln^{3+})$$

Where, $c(Ln^{3+})$ is a fraction of activator dopant ions within a given LnNP core.

According to these considerations and taking the # of Nd^{3+} ions equal to 1 in 5 mol% Nd^{3+}-doped LnNPs, the 12.5 and 25 mol% Nd^{3+}-doped LnNPs had 2.15 and 3.89 times more of Nd^{3+}, respectively.

Nd^{3+}-doped LnNPs – PLQY Comparison

Table S2. PLQY comparison of different Nd^{3+}-doped LnNPs. N/R – information is not reported. In the case of relative PLQY determination, references were: *indocynine green dye in DMSO, **$NaGdF_4$: 3 mol% Nd^{3+}/$NaGdF_4$ LnNPs in hexane, #IR26 in 1, 2-dichloroethane.

Composition of LnNPs	*Size*, nm	*Media*	*Method*	*PLQY*, % @ P_d, W/cm^2	REF
YF_3: 5 mol% Nd^{3+}	19 ± 4 nm	Powder	Decay rates	~1%	Tan et al.[3]
LaF_3: 0.5 mol% Nd^{3+}	5 - 15 nm	Powder	Decay rates	88%	Cui et al.[4]
$NaGdF_4$: 3 mol% Nd^{3+}	~11 nm	Hexane	Relative*	22%	Chen et al.[5]
$NaGdF_4$: 3 mol% Nd^{3+}/$NaGdF_4$	~15 nm	Hexane	Relative*	40%	
		Water	Relative**	20%	
LaF_4: 3 mol% Nd^{3+}/LaF_3	N/R	N/R	Thermal lens	70%	Rocha et al.[6]
Fluorapatite: 1 mol% Nd^{3+}	N/R	N/R	Absolute	~8% @1060 nm	Karthi et al.[7]
$LiLuF_4$: 10 mol% Nd^{3+}/$LiLuF_4$	35.6×31.9 nm	Hexane	Absolute	32%	Qin et al.[8]
$NaGdF_4$: 5 mol% Nd^{3+}/$NaGdF_4$	8 nm	N/R	N/R	15.63 ± 0.06% @1060 nm	Wang et al.[9]
		Water		13.21 ± 0.05% @1060 nm	
$NaGdF_4$: 5 mol% Nd^{3+}/$NaGdF_4$	24.6 ± 1.2 nm	Water	Relative#	0.36% @1057 nm 0.16% @1335 nm	Ren et al.[10]
$NaGdF_4$: 5 mol% Nd^{3+}/$NaGdF_4$	25.3 ± 0.7 nm	Hexane	Absolute	17.4 ± 2.5%	This work
		Water		8.8 ± 0.9%	

References

(1) Boyer, J.-C.; Vetrone, F.; Cuccia, L. A.; Capobianco, J. A. Synthesis of Colloidal Upconverting $NaYF_4$ Nanocrystals Doped with Er^{3+}, Yb^{3+} and Tm^{3+}, Yb^{3+} via Thermal Decomposition of Lanthanide Trifluoroacetate Precursors. *J. Am. Chem. Soc.* **2006**, *128* (23), 7444–7445.

(2) Bogdan, N.; Vetrone, F.; Ozin, G. A.; Capobianco, J. A. Synthesis of Ligand-Free Colloidally Stable Water Dispersible Brightly Luminescent Lanthanide-Doped Upconverting Nanoparticles. *Nano Lett.* **2011**, *11* (2), 835–840.

(3) Tan, M. C.; Kumar, G. A.; Riman, R. E.; Brik, M. G.; Brown, E.; Hommerich, U. Synthesis and Optical Properties of Infrared-Emitting YF_3:Nd Nanoparticles. *J. Appl. Phys.* **2009**, *106* (6), 063118.

(4) Cui, X.; She, J.; Cui, K.; Gao, C.; Hou, C.; Wei, W.; Peng, B. Nd^{3+}-Doped LaF_3 Nanoparticles with a Larger Emission Cross-Section. *Chem. Phys. Lett.* **2010**, *489* (4–6), 191–194.

(5) Chen, G.; Ohulchanskyy, T. Y.; Liu, S.; Law, W.-C.; Wu, F.; Swihart, M. T.; Ågren, H.; Prasad, P. N. Core/Shell $NaGdF_4$:Nd^{3+}/$NaGdF_4$ Nanocrystals with Efficient Near-Infrared to Near-Infrared Downconversion Photoluminescence for Bioimaging Applications. *ACS Nano* **2012**, *6* (4), 2969–2977.

(6) Rocha, U.; Jacinto da Silva, C.; Ferreira Silva, W.; Guedes, I.; Benayas, A.; Martínez Maestro, L.; Acosta Elias, M.; Bovero, E.; van Veggel, F. C. J. M.; García Solé, J. A.; Jaque, D. Subtissue Thermal Sensing Based on Neodymium-Doped LaF_3 Nanoparticles. *ACS Nano* **2013**, *7* (2), 1188–1199.

(7) Karthi, S.; Kumar, G. A.; Sardar, D. K.; Santhosh, C.; Girija, E. K. Synthesis and Characterization of Nd^{3+}: Yb^{3+} Co-Doped near Infrared Sensitive Fluorapatite Nanoparticles as a Bioimaging Probe. *Opt. Mater.* **2018**, *77*, 39–47.

(8) Qin, Q.-S.; Zhang, P.-Z.; Sun, L.-D.; Shi, S.; Chen, N.-X.; Dong, H.; Zheng, X.-Y.; Li, L.-M.; Yan, C.-H. Ultralow-Power near-Infrared Excited Neodymium-Doped Nanoparticles for Long-Term in Vivo Bioimaging. *Nanoscale* **2017**, *9* (14), 4660–4664.

(9) Wang, P.; Jiang, S.; Li, Y.; Luo, Q.; Lin, J.; Hu, L.; Fan, L. Downshifting Nanoprobes with Follicle Stimulating Hormone Peptide Fabrication for Highly Efficient NIR II Fluorescent Bioimaging Guided Ovarian Tumor Surgery. *Nanomedicine Nanotechnol. Biol. Med.* **2020**, 102198.

(10) Ren, Y.; He, S.; Huttad, L.; Chua, M.-S.; So, S. K.; Guo, Q.; Cheng, Z. NIR-II/MR Dual Modal Nanoprobe for Liver Cancer Imaging. *Nanoscale* **2020,** *12,* 11510-11517.